# Data-Driven Modeling and Prediction of the Process for Selecting Runway Configurations

Jacob Avery and Hamsa Balakrishnan

**Runway configuration is a key driver of airport capacity at any time. Several factors, such as wind speed and direction, visibility, traffic demand, air traffic controller workload, and the coordination of flows with neighboring airports, influence the selection of the runway configuration. This paper infers the utility functions of the nominal decision-making process of air traffic personnel by using a discrete choice modeling approach. Given operational and weather conditions that have already been reported, such as ceiling and visibility, traffic demand, and current runway configuration, the model produces a probabilistic forecast of the runway configuration on a 15-min horizon. The prediction is then extended to a more realistic 3-h planning horizon. Case studies for San Francisco (SFO), California; LaGuardia (LGA), New York; and Newark (EWR), New Jersey, airports were completed by using this approach. Given the weather and airport arrival demand, the model predicts the correct runway configuration at SFO, LGA, and EWR on a 3-h horizon with accuracies of 81.2%, 81.3%, and 77.8%, respectively.**

Airport congestion leads to significant flight delays at the busiest airports in the United States. Fundamentally, congestion is caused by an imbalance between demand (airport operations) and supply (airport capacity) within the air transportation system. Airport expansion projects can increase airport capacity but are expensive and take many years to complete; by contrast, better utilization of existing airport capacity is a less expensive approach to mitigating congestion. The key driver of airport capacity at a given time is the active runway configuration, which is the combination of runways being used to handle the arrival and departure flows at the airport under consideration (*1*).

When a runway configuration is being selected, air traffic controllers must consider meteorological and operational factors, such as wind speed and direction, arrival and departure demand, noise mitigation, and interairport coordination. A comprehensive understanding of the process for selecting runway configurations by air traffic personnel is necessary for the development of decision support tools under the initiatives of the Single European Sky Air Traffic Management Research (SESAR) and the Next-Generation Air Transportation System (NexGen). A keen understanding of this process has the potential to increase operational efficiency of airport capacity utilization and provides a key step toward prediction of airport capacity. Prediction of capacity can act as a supplement to predicting, and even reducing, air traffic delays.

Massachusetts Institute of Technology, 77 Massachusetts Avenue, 33-328, Cambridge, MA 02139. Corresponding author: J. Avery, avery2@mit.edu.

*Transportation Research Record: Journal of the Transportation Research Board, No. 2600,* Transportation Research Board, Washington, D.C., 2016, pp. 1–11.
DOI: 10.3141/2600-01

This paper uses a data-driven approach to model the runway configuration selection process by using a discrete choice modeling framework for LaGuardia (LGA), New York City; San Francisco (SFO), California; and Newark (EWR), New Jersey, airports. The model infers the utility functions that best explain (i.e., maximize the likelihood of ) the observed decisions. The utility functions give insight to the relative importance of the different decision factors to air traffic control when a runway configuration is being selected. The resultant model also yields a probabilistic prediction of the runway configuration at any time, given a forecast of the influencing factors.

## PREVIOUS WORK

Two types of models have previously been developed for the problem of runway configuration selection: prescriptive models and descriptive models. Prescriptive models account for the weather and other operational constraints to recommend an optimal runway configuration. Examples include the enhanced preferential runway advisory system (ENPRAS) for optimal runway configuration selection (*2*), runway allocation systems at both Sydney and Brisbane, Australia, airports (*3*), and the more recent models for scheduling runway configurations that account for weather forecasts and capacity loss during runway switches (*4*–*8*). These models have proven effective to optimize the system but are limited when they attempt to describe the decision-making process itself.

Descriptive models use data mining approaches to predict the selection of runway configuration on the basis of historical data. These models make predictions from the selection process of decision makers themselves rather than by recommending an optimal configuration. Examples include the forecasting of airport arrival rates during ground delay programs (*9, 10*), the forecasting of the selection of runway configuration at Amsterdam Schiphol Airport on a 24-h prediction horizon by using probabilistic weather forecasts (*11*), and models for logistic regression of the selection of runway configurations for John F. Kennedy International (JFK) and LGA Airports (*12*). These models have shown accuracies of up to 75%; however, a difficult task has been quantifying the observed resistance to configuration switches by air traffic control, called "operational inertia" in this paper. Switching a runway configuration requires increased coordination among airport stakeholders, a maneuver that lowers airport throughput. Consequently, runway configuration switches typically occur less frequently per day than what would be optimal. A discrete choice approach has the advantage of accounting for inertia within its weighted variables and predictions.

More recently, discrete choice models of the process for selecting runway configurations have been created for 2006 at LGA and EWR

(*13, 14*). This paper will extend these models at LGA and EWR data for 2011 and 2012 with a more data-driven approach. The methodology will also be applied to SFO for 2011 and 2012. A key novelty of this paper is that the constraints pertaining to the maximum allowable tailwinds and crosswinds are learned from the actual data rather than from FAA operating manuals.

## NOTATION

Runway configurations are typically designated in the form A1, A2|D1, D2, for which A1 and A2 are the arrival runways and D1 and D2 are the departure runways. The numbers for each active runway are reported on the basis of their bearing in degrees from magnetic north divided by 10. Parallel runway pairs are designated by an R (right) and L (left) after their numbers. For instance, if SFO (Figure 1) is operating in runway configuration 28L|1R, 1L, aircraft arrivals are handled on runway 28L, which faces 280° from magnetic north, and departures are handled on both parallel runways 1R and 1L, which face 10° from magnetic north.

## METHODOLOGY

### Framework for Discrete Choice Modeling

Discrete choice models are behavioral models that describe the choice selection of an individual decision maker, or the nominal decision selection among an exhaustive set of possible alternatives called the "choice set" (*15*). Each alternative in the choice set is assigned a utility function on the basis of the attributes related to the decision-making process. At a given time, the feasible alternative with the maximum utility value is taken as the decision in the model.

The utility function $U$ is modeled as a stochastic random variable with an observed deterministic component, $V$, and a stochastic error component, $\varepsilon$. For the $n$th decision selection, given a set of feasible alternatives, $C_n$, the utility of choice, $c_i \in C_n$ is represented as

$$U_{n,i} = V_{n,i} + \varepsilon_{n,i} \tag{1}$$

where $i$ is a specific alternative from 1, 2, . . . , $n$.

The observable component of the utility function is defined as a linear function of the observed vector of attributes, $\vec{X}_{n,i}$. The attributes include the different factors that can influence the decision. They are weighted by the values in vector $\vec{\beta}_{n,i}$ and include alternative specific constants $\alpha_{n,i}$ as follows:

$$V_{n,i} = \alpha_{n,i} + \left[\vec{X}_{n,i} \cdot \vec{\beta}_{n,i}\right] \tag{2}$$

The random error component of the utility function reflects all measurement errors, including unobserved attributes, variations between different decision makers, proxy variable effects, and reporting errors. The error term is assumed to be distributed according to a Type I extreme value (or Gumbel) distribution with a location parameter of zero. The Gumbel distribution is used to approximate a normal distribution due to its computational advantages. The multinomial logit (MNL) model structure assumes that the error components of each utility function are independent from one another. Under the assumptions of the MNL model, the probability $P$ that choice $c_i$ is chosen during the $n$th decision selection period is given by Equation 3:

$$P_{n,i} = \frac{\exp\left(V_{n,i}\right)}{\sum_{j:c_j \in C_n} \left[\exp\left(V_{n,j}\right)\right]} \tag{3}$$

where $j$ is an alternative from 1, 2, . . . , $n$.

The independence among the error terms of each utility function in the MNL model assumes that all correlation among alternatives has been captured by the attributes included in the utility function (*15*). The nested logit (NL) model relaxes this assumption by grouping alternatives into subsets, or nests (denoted $B_k$), that have correlation between their error terms. NL models are typically illustrated by a tree diagram.

The NL model splits the observable part of the utility function into a component that is common among the alternatives within a nest and a component that varies between the different alternatives in a nest. The NL model can then be treated as nested MNL models by using conditional probabilities. The probability that a specific alternative is chosen is given by the probability that a specific alternative nest is

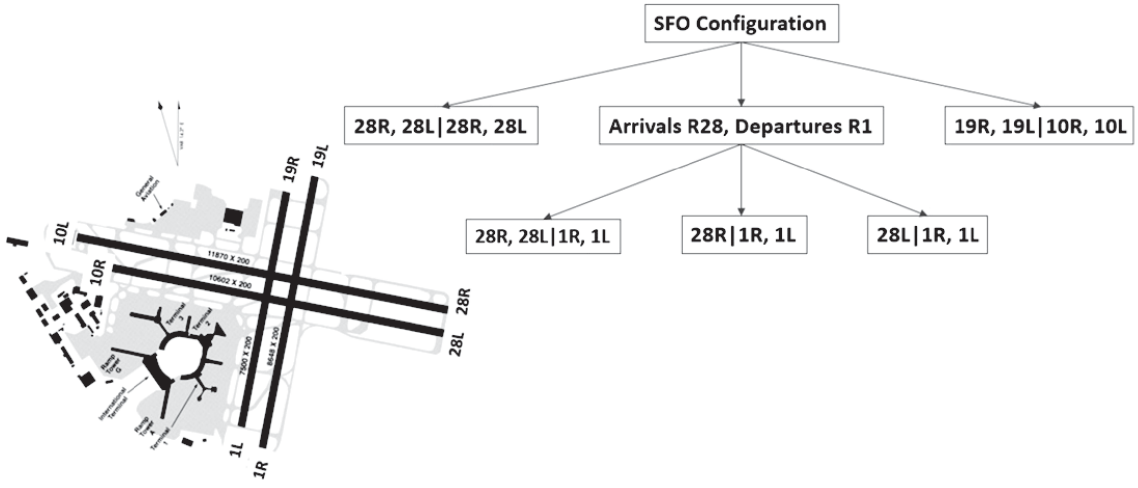


FIGURE 1 SFO model specification.

chosen multiplied by the probability that the specific alternative is chosen from among the alternatives in that nest. In other words

$$P_n(c_i) = P_n(c_i|B_k)P_n(B_k) \tag{4}$$

$$P_n(B_k) = \frac{\exp(I_{n,k})}{\sum_{l=1}^{K}[\exp(I_{n,l})]} \tag{5}$$

$$P_n(c_i|B_k) = \frac{\exp(\mu_k V_{n,i})}{\sum_{j\in B_k}[\exp(\mu_k V_{n,j})]} \tag{6}$$

$$I_{n,k} = \frac{1}{\mu_k}\ln\left(\sum_{j\in B_k}[\exp(\mu_k V_{n,i})]\right) \tag{7}$$

where

$k$ = nest between 1, 2, . . . , $K$;
$l$ = nest between 1, 2, . . . , $K$; and
$\mu$ = scale parameter for a nest.

Equation 5 has an additional term in the numerator, the "inclusive value," that acts as a bridge between the lower-level MNL models within each nest and the upper-level ones.

## Maximum Likelihood Estimation

Maximum likelihood estimates of the linear weighting parameters, alternative specific constants, and scale parameters are estimated from the training data. The maximum likelihood function $\mathcal{L}$ is the joint probability that the vector of sample data ($\vec{\theta}$) will occur given a vector of parameters $\vec{\theta} = <\alpha, \vec{\beta}, \mu>$ as follows:

$$\mathcal{L}(\vec{\theta}) = P\{\vec{X}, \vec{\theta}\} \tag{8}$$

The estimated parameters $\hat{\alpha}$, $\hat{\beta}$, $\hat{\mu}$ are those that maximize the likelihood of the observations:

$$(\hat{\alpha}, \hat{\beta}, \hat{\mu}) = \max(\mathcal{L}(\alpha, \vec{\beta}, \mu))$$

The resulting nonlinear optimization problem is solved computationally by using the open-source software package Biogeme (*16*).

## Statistical Testing

The discrete choice models for SFO, LGA, and EWR were realized iteratively by adding or removing variables on the basis of their statistical significance as determined by the Student's *t*-test. The significance of each attribute to the overall model was tested by using likelihood ratio testing. Different NL model tree structures were also evaluated for statistical significance by using likelihood ratio testing (*15*).

## Prediction Model

The utility functions from the discrete-choice model are applied in Equations 4 to 7 to develop the probabilities of selecting each runway configuration during a given 15-min interval. For a 15-min horizon, the runway configuration with the maximum positive utility (and therefore maximum probability of selection) is taken as the predicted decision. For a 3-h prediction horizon, all possible evolutions of the runway configuration selection for the next 3 h (in 15-min intervals) must be considered. Here, Bayes' rule was recursively applied at each 15-min interval to determine the probabilities of a runway configuration selection on a 3-h prediction horizon (*17*). In the prediction models, "accuracy" was defined as the percentage of time that the observed configurations were correctly predicted.

## Training and Test Data

The training and test data sets for each airport were taken from the FAA's Aviation System Performance Metrics (ASPM) database (*18*). The data are reported in 15-min intervals and include the active runway configuration, the arrival and departure demand, cloud ceiling, visibility conditions, and wind speed and direction. Training data for SFO, LGA, and EWR were taken from 2011, and the test data sets were taken from 2012. Because the ASPM data were used in the estimated models for the prediction, that prediction assumes perfect knowledge of the wind, visibility, and demand for the subsequent 3 h. Future work may evaluate the effects of forecast weather data into the predictions.

## Runway Configuration Filtering

Runway configurations that were seen less than 1% of the time throughout the year were removed at SFO and EWR to reduce possible reporting errors or cases of special operations that make difficult the reliable estimating and predicting of the models. For LGA, the filter was set to 2% to help further reduce errors that occurred during the nighttime hours. Table 1 shows the most common configurations at SFO, LGA, and EWR from the 2011 data after filtering.

**TABLE 1 Configurations Observed at SFO, LGA, and EWR in 2011**

| Airport | Designation | Configuration (Arrival\|Departure) | Frequency | Percentage of Frequency |
|---|---|---|---|---|
| SFO | 1 | 19R, 19L\|10R, 10L | 957 | 3 |
| | 2 | 28R, 28L\|1R, 1L | 24,871 | 74 |
| | 4 | 28R, 28L\|28R, 28L | 3,000 | 9 |
| | 5 | 28R\|1R, 1L | 467 | 1 |
| | 6 | 28L\|1R, 1L | 4,244 | 13 |
| LGA | 1 | 22\|13 | 6,846 | 24 |
| | 2 | 22\|31 | 5,556 | 19 |
| | 3 | 22, 31\|31 | 852 | 3 |
| | 4 | 31\|31 | 2,676 | 9 |
| | 5 | 31\|4 | 7,608 | 26 |
| | 6 | 4\|13 | 4,113 | 14 |
| | 7 | 4\|4 | 1,372 | 5 |
| EWR | 1 | 22L, 11\|22R | 4,214 | 13 |
| | 2 | 22L\|22R | 16,559 | 50 |
| | 3 | 22L\|22R, 29 | 353 | 1 |
| | 4 | 4L, 4R\|4L | 528 | 2 |
| | 5 | 4R, 11\|4L | 1,576 | 5 |
| | 6 | 4R\|4L | 10,221 | 31 |

## ATTRIBUTE SELECTION AND VARIABLE PROCESSING

### Inertia

"Operational inertia" is a term used to describe the observed resistance of air traffic controllers to resist configuration changes because of the high operational effort required to switch to a different runway configuration. Tools designed to suggest an optimal runway configuration have been shown to recommend significantly more frequent runway configuration switches than are observed in practice. An inertia variable was added as an attribute to reflect the preference of air traffic controllers to hold the same runway configuration as long as operationally safe; such changes require, between all stakeholders, increased coordination that would reduce airport throughput (*7*). The inertia variable adds a positive contribution to a runway configuration's utility if that same configuration is used in the previous time interval.

### Wind Speed and Direction

Wind speed and direction are key factors that influence the choice of runway configuration. High tailwinds and crosswinds are operationally unsafe in many circumstances, and, as a result, render certain runways unusable. The FAA has specified the maximum allowable tailwind and crosswind values for the operation of a runway in standard operating procedures. Prior work on selection of runway configuration had based runway availability on standard operating procedures; however, in this paper, threshold values are removed from the 2011 ASPM data sets.

Figure 2 shows the observed wind speed and direction combinations for 2011 at SFO, LGA, and EWR on a wind rose. In the figure, the solid lines correspond to the maximum thresholds, and the colors indicate the frequency of occurrence of different points. The identified ranges of tailwind and crosswind values for runway feasibility were learned directly from the 2011 ASPM data and are also shown on the plot. Air traffic controllers prefer headwinds to tailwinds and crosswinds, and while no headwind threshold exists for runway feasibility, headwind thresholds were plotted at 40 knots for a better illustration. The tailwind and crosswind limits were taken on a per-runway basis and calculated via the following procedure:

1. Aggregate all tailwind and crosswind values for each runway at SFO, LGA, and EWR.
2. For each runway list, remove tailwind and crosswind combinations from periods when the active configurations did not include any operations on the runway.
3. Take tailwind and crosswind thresholds at the 98th percentile to remove possible reporting errors.

The available choice set during a given decision selection period can change in a discrete choice framework. Runway feasibility was used to govern directly the available subset of runway configurations in the discrete choice model during a given interval. If the wind speed and direction combination fell outside the thresholds for a runway, all configurations using that runway were removed from the available choice set during the given decision selection period. Figure 2 shows that the majority of points correspond to conditions for which all the runway configurations are considered feasible.

Headwinds are expected to add a positive contribution to the utility functions, and tailwinds are expected to add a negative contribution. Significantly high headwinds, however, could potentially have an adverse effect on airport operations by decreasing the space between aircraft arrivals during landing, a phenomenon known as "compression" (*19*). To account for the effects of compression, headwinds above the 85th percentile were treated as high headwinds. Variables for normal headwinds (below the 85th percentile) and tailwinds were added in each model as well.

### Demand

Airport arrival and departure demand play a significant role when the runway configuration is being selected. Specifically, in high-demand situations, high-capacity configurations are preferred. These typically include an extra arrival or departure runway.

### Noise Abatement Procedures

Noise abatement procedures are used at many major airports to reduce the impacts of noise on communities in the vicinity of the airport, especially during early-morning and nighttime hours. At SFO, runway configurations that require arrivals and departures over water are preferred to those that require flying over populated areas. At LGA, configurations with flight paths over the city and away from populated areas are preferred during nighttime. Variables were included in each model to account for these effects.

### Cloud Ceiling and Visibility

Cloud ceiling and visibility are important for air traffic control when the runway configuration is being selected. The term "visual meteorological conditions" (VMC) refers to times when the visibility is sufficient for pilots to maintain visual separation from the ground and other aircraft, while the term "instrument meteorological conditions" (IMC) refers to times when pilots are required to use their flight instruments. The selection of runway configuration could depend on whether VMC or IMC is implemented. In addition, airport capacity is higher in VMC than in IMC because IMC requires increased aircraft separations. Categorical variables were added to each model to account for VMC and IMC.

### Coordination with Neighboring Airports in New York City Metroplex

The four airports in the New York City metroplex—LGA, EWR, John F. Kennedy International (JFK), and Teterboro (TEB)—are in close proximity to one another. Air traffic controllers at each airport must therefore coordinate their aircraft arrival and departure flows with the other airports. In the LGA and EWR models, the impacts of TEB were ignored and categorical variables were added to account for operations at JFK. JFK was included here because of its large volume of operations, which was assumed to have a significant impact on the runway configurations at LGA and EWR.

### Switch Proximity

If airport conditions necessitate a runway configuration switch, certain such switches require more coordination from airport

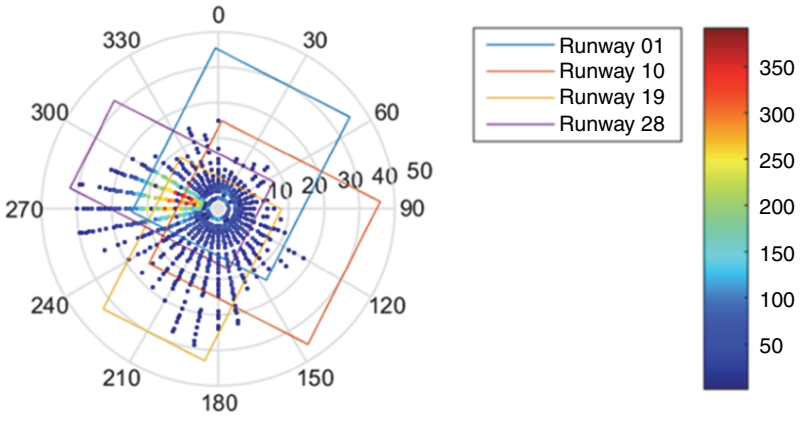


(a)

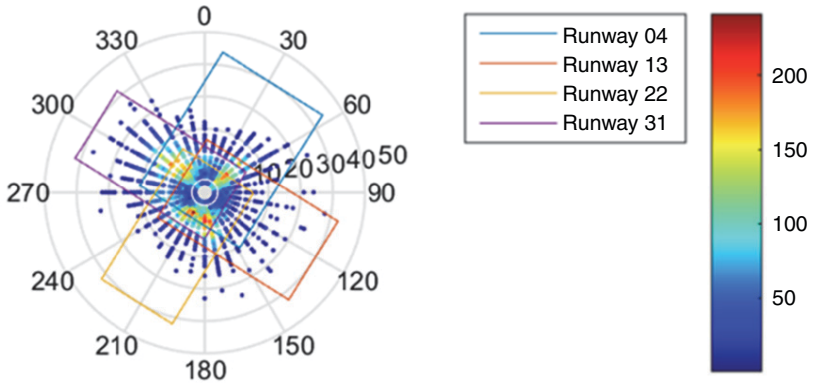


(b)

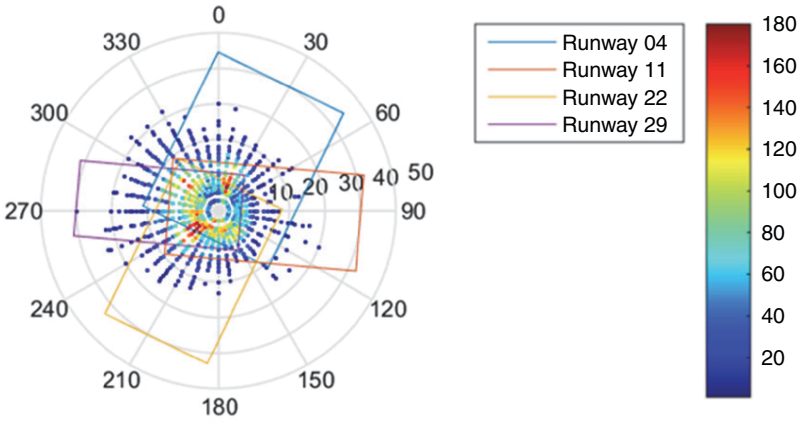


(c)

FIGURE 2 Wind speeds and directions observed in 2011 at (*a*) SFO, (*b*) LGA, and (*c*) EWR.

stakeholders than others. For instance, the addition of an extra arrival runway may be easier to implement than a complete reversal in the direction of operations. To account for these effects, variables were added to weight each utility function differently in relation to the previous configuration. The switch proximity variables are fundamentally the same as the inertia variables but are applied only to the utility functions of the runway configurations that were not seen in the previous time interval. In this sense, switch proximity variables do not account for the resistance of switching a runway configuration in general; rather, they account for the low likelihood of switching between two runway configurations, which requires a high amount of operational effort once the decision to switch has been made.

### Special Considerations for SFO

The optimal capacity configuration at SFO is 28R, 28L|1R, 1L. The runways used in this operation are closely spaced, at 750 ft apart. FAA regulations specify that simultaneous arrivals are not allowed under IMC conditions (*20*). Therefore, one would expect that the 28R|1R, 1L or the 28L|1R, 1L configuration (which involves using only one of the two runways for arrivals) would be favored under IMC; however, the ASPM data suggest that configuration 28R, 28L|1R, 1L was used 19,832 (82.7%) times under VMC and 4,161 (17.3%) times under IMC and that configurations 28R|1R, 1L and 28L|1R, 1L were used 3,466 (65.3%) times under VMC and 1,844 (34.7%) times under IMC. Even though the configurations with a single arrival runway were used a greater fraction of the time in IMC than in VMC, the runway configuration 28R, 28L|1R, 1L was still used a majority of the time in IMC. Under IMC, simultaneous side-by-side landings are not possible, and the airport operates as if it would be in a configuration with a single arrival runway by using a staggered-arrival approach. Operationally, the staggered 28R, 28L|1R, 1L configuration under IMC may have a small capacity benefit over the 28R|1R, 1L and 28L|1R, 1L configurations. To evaluate these effects, new variables that combine the effects of visibility and demand were used in the SFO model. Four categorical variables were defined for periods of

1. IMC + low demand,
2. IMC + high demand,
3. VMC + low demand, and
4. VMC + high demand.

In these cases, a "low demand" was defined as less than five arrivals per 15-min period and "high demand" was defined as greater than eight arrivals per 15-min period.

## CASE STUDY: SFO

### Model Specification

In the SFO model, configurations were removed if they were not seen in at least 1% of the decision selection periods throughout the year. As shown in Figure 1, the chosen model had a nested logit structure with six possible alternative runway configurations. The model structure grouped similar configurations 28R, 28L|1R, 1L, 28L|1R, 1L and 28R|1R, 1L into a common nest with scale parameter $\mu_{ARR28DEP1} = 1.16$. The other two configurations were modeled as singleton nests.

### Estimated Model and Inferences

The estimated weighting parameters for the utility function for the SFO model are shown in Table 2, which includes the estimated value, the standard error, and the *t*-statistics. Any parameter that was not statistically significant (i.e., the *t*-statistic had an estimated value less than 1.96) was removed from the model, except in cases for which removing the variable would bias the predictions.

Table 2 shows that the inertia variables were the most important ones in the decision selection. All configurations within the nest have the same inertia value because they were modeled under a common inertia variable. Because of the VMC–IMC reporting challenges noted earlier, the extreme sensitivity of these configurations to the biases in the prediction model made the choice of the same inertia value necessary.

Wind was another significant factor for the SFO decision selection. During estimation, compression did not show a significant influence on the high headwind attributes. Furthermore, headwinds and tailwinds were linearly correlated. Therefore, as the values in Table 2 show, these variables were constrained linearly for the final model. Figure 1 shows that the wind at SFO is predominantly from the San Bruno Gap and corresponds to a headwind for arrivals on runway 28. Five of the six unique configurations in the SFO model serve arrivals by using Runways 28R and 28L because of this headwind advantage. During poor weather conditions, low pressure sys-

**TABLE 2 Estimated Utility Function Weights for SFO**

| Parameter | Value | SE | *t*-Stat. |
|---|---|---|---|
| Inertia Parameters | | | |
| Configuration 19R, 19L\|10R, 10L | 3.20 | 0.376 | 8.64 |
| Configuration 28R, 28L\|1R, 1L | 4.48 | 0.139 | 31.87 |
| Configuration 28R, 28L\|28R, 28L | 4.35 | 0.209 | 20.82 |
| Configuration 28R\|1R, 1L | 4.48 | 0.139 | 31.87 |
| Configuration 28L\|1R, 1L | 4.48 | 0.139 | 31.87 |
| Wind Parameters | | | |
| High headwind on arrival runway | 0.0415 | 0.0131 | 3.20 |
| Normal headwind on arrival runway | 0.0415 | 0.0131 | 3.20 |
| Tailwind on arrival runway | –0.0415 | 0.0131 | –3.20 |
| High headwind on departure runway | 0.0608 | 0.0076 | 8.14 |
| Normal headwind on departure runway | 0.0608 | 0.0076 | 8.14 |
| Tailwind on departure runway | –0.0608 | 0.0076 | 8.14 |
| Demand–Visibility Parameters | | | |
| VMC + high demand; 28R/L\|1R, 1L | –1.66 | 0.39 | –3.44 |
| IMC + low demand; 28R/L\|1R, 1L | 0.327 | 0.381 | 0.93 |
| Switch Proximity Parameters | | | |
| 28R, 28L\|1R, 1L to 28R, 28L\|28R, 28L | –1.2 | 0.189 | –5.98 |
| 28R/L\|1R, 1L to 28R, 28L\|28R, 28L | –1.2 | 0.189 | –5.98 |
| 19R, 19L\|10R, 10L to 28R, 28L\|1R, 1L | –0.775 | 0.649 | –1.22 |
| 19R, 19L\|10R, 10L to 28R/L\|1R, 1L | –0.775 | 0.649 | –1.22 |
| 19R, 19L\|10R, 10L to 28R, 28L\|28R, 28L | –0.946 | 0.601 | –1.57 |
| 28R, 28L\|28R, 28L to 28R, 28L\|1R, 1L | 1.33 | 0.251 | 4.97 |
| 28R, 28L\|28R, 28L to 28R\|/L 1R, 1L | 1.33 | 0.251 | 4.97 |
| Noise Abatement Parameters | | | |
| Depart Runway 28 during evening | –0.356 | 0.176 | –3.23 |
| Arrive Runway 10 during evening | –0.356 | 0.176 | –3.23 |

tems with high circulating winds disrupt the typical pattern, making runway configuration 19R, 19L|10R, 10L more attractive for air traffic control (*21*). As a consequence, the headwind variables in the model are predominantly used to distinguish between runway configuration options with arrivals on the Runways 28 or on the Runways 19.

In the SFO model, attributes that grouped the effects of demand and visibility were estimated. As Table 2 shows, the utility function for 28R|1R, 1L and 28R|1R, 1L received a negative demand bonus under VMC and a positive demand bonus under IMC. In addition, the noise parameters indicated that flights over water during the evening hours are preferred to flights departing over nearby communities. This preference seems to coincide with noise abatement procedures at SFO (*22*) and would likely be more prevalent if other configurations such as 28R, 28L|10R, 10L were modeled in the future.

The switch proximity variables also showed statistically significant effects in the SFO model. In particular, the estimated coefficients reflected a preference to switch from runway Configuration 28R, 28L|28R, 28L, which is likely because this configuration is used primarily for long-haul arrivals and departures that fly over the Pacific Ocean. In addition, Configuration 19R, 19L|10R, 10L does not show a preference to revert to the configurations with arrivals on Runways 28 perhaps because the 19R, 19L|10R, 10L configuration would be used during significant shifts in wind patterns over the San Bruno Gap.

### Prediction of Runway Configuration

A challenge at SFO is accurately predicting between Configuration 28R, 28L|1R, 1L with arrivals on the closely spaced parallel runways and the Configurations 28R|1R, 1L and 28L|1R, 1L, with single arrival runways. As noted earlier, simultaneous (side-by-side) landings are not possible under IMC, and the airport operates almost as it would in a configuration with a single arrival runway, even in 28R, 28L|1R, 1L. The reported configurations in the ASPM data set do not differentiate between simultaneous and staggered parallel approaches, even though staggered approaches have a capacity that would be closer to 28R|1R, 1L or 28L|1R, 1L. This fact, along with the other similarities between these two runway configuration alternatives, makes it difficult to predict either of these alternatives accurately without introducing a selection bias. Accurately predicting 28R, 28L|28R, 28L is also challenging because of the limitations from the ASPM data set. This runway configuration is typically used only for long-haul departures over the Pacific Ocean and to Hawaii, and the aggregate flight counts in ASPM are not sufficient to account for this factor. Despite these challenges, the overall prediction accuracy in 2012 for SFO on a 15-min prediction horizon was 98.2% and on a 3-h prediction horizon was 81.2%, under the assumption of perfect knowledge of future weather conditions and traffic demand. The accuracy of individual configuration predictions is shown in Table 3. Configurations that were seen more infrequently had lower relative prediction accuracies.

TABLE 3 Prediction Accuracy for SFO in 2012 for 15-min and 3-h Prediction Horizons

| Configuration (Arrival\|Departure) | Frequency | Prediction Accuracy (%) | |
|---|---|---|---|
| | | 15 min | 3 h |
| 19R, 19L\|10R, 10L | 1,145 (4%) | 98.9 | 86.7 |
| 28R, 28L\|1R, 1L | 22,641 (71%) | 98.7 | 88.6 |
| 28R, 28L\|28R, 28L | 2,952 (9%) | 97.8 | 55.3 |
| 28R\|1R, 1L | 925 (3%) | 93.1 | 51.7 |
| 28L\|1R, 1L | 4,123 (13%) | 96.3 | 64.8 |
| Total | 31,786 | 98.2 | 81.2 |

## CASE STUDY: LGA

### Model Specification

In the LGA model, configurations were removed if they were not seen in at least 2% of the decision selection periods throughout the year. Many model structures were tested, and the final resulting model was chosen as a nested logit structure with a single nest containing all alternatives that used Runway 22 for arrivals with a scale parameter of $\mu_{ARR22} = 1.1$, shown in Figure 3.

### Estimated Model and Inferences

The estimated weighting parameters for the utility function for the LGA model are shown in Table 4. As with the SFO model, here

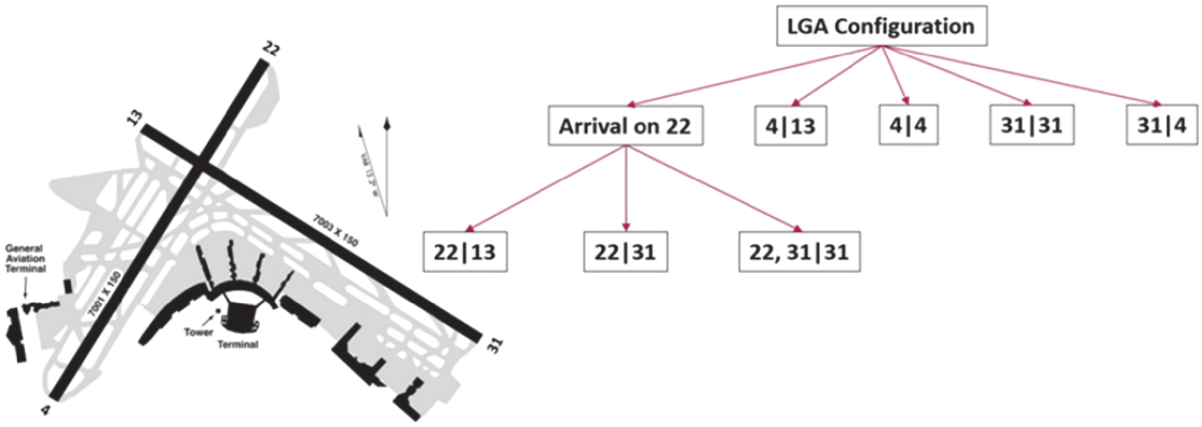


FIGURE 3 LGA model specification.

**TABLE 4 Estimated Utility Function Weights for LGA**

| Parameter | Value | SE | *t*-Stat. |
|---|---|---|---|
| Inertia Parameters | | | |
| Configuration 22\|13 | 4.58 | 0.187 | 24.5 |
| Configuration 22\|31 | 7.41 | 0.36 | 20.57 |
| Configuration 22,31\|31 | 7.41 | 0.36 | 20.57 |
| Configuration 31\|31 | 4.91 | 0.401 | 12.24 |
| Configuration 31\|4 | 3.16 | 0.25 | 12.6 |
| Configuration 4\|13 | 3.99 | 0.196 | 20.34 |
| Configuration 4\|4 | 5.44 | 0.416 | 13.1 |
| Wind Parameters | | | |
| High headwind on arrival runway | 0.0952 | 0.0161 | 5.89 |
| Normal headwind on arrival runway | 0.123 | 0.0197 | 6.26 |
| Tailwind on arrival runway | –0.0946 | 0.0199 | –4.74 |
| Tailwind on departure runway | –0.211 | 0.0173 | –12.2 |
| Tailwind on extra arrival runway | –0.348 | 0.07 | –4.97 |
| Demand Parameters | | | |
| Arrival demand: 31\|31 | –0.101 | 0.0312 | –3.24 |
| Arrival demand: 4\|4 | –0.0807 | 0.0327 | –2.47 |
| VMC–IMC Parameters | | | |
| VMC on 31\|31 | 2.09 | 0.402 | 5.19 |
| VMC on 31\|4 | 1.36 | 0.231 | 5.9 |
| Switch Proximity Parameters | | | |
| 31\|4 to 31\|31 | –1.4 | 0.463 | –3.03 |
| 4\|13 to 31\|31 | –2.52 | 0.714 | –3.53 |
| 4\|4 to 31\|31 | –1.22 | 0.747 | –1.77 |
| 22\|13 to 31\|31 | –1.99 | 0.577 | –3.45 |
| 4\|13 to 31\|4 | –2.19 | 0.368 | –5.94 |
| 4\|4 to 31\|4 | –1.05 | 0.515 | –2.04 |
| 22\|13 to 31\|4 | –2.14 | 0.355 | –6.04 |
| 4\|13 to 4\|4 | –1.6 | 0.443 | –3.61 |
| 22\|13 to 4\|4 | –1.92 | 0.532 | –3.6 |
| 31\|31 to 22\|13 | –1.05 | 0.573 | –1.84 |
| Interairport Coordination Parameters | | | |
| LGA departures on runway 4 vs. JFK arrivals on runway 13 | 0.85 | 0.308 | 2.76 |
| LGA departures on runway 13 vs. JFK arrivals on runway 13 | 1.27 | 0.464 | 2.75 |
| LGA departures on runway 31 vs. JFK departures on runway 13 | –1.99 | 0.224 | –8.88 |
| LGA departures on runway 22 vs. JFK arrivals on runway 13 | –0.448 | 0.172 | –2.6 |
| LGA departures on runway 31 vs. JFK arrivals on runway 13 | –1.61 | 0.222 | –7.26 |
| LGA departures on runway 13 vs. JFK arrivals on runway 13 | 0.796 | 0.25 | 3.19 |
| LGA departures on runway 31 vs. JFK departures on runway 4 | –2.5 | 0.341 | –7.34 |
| LGA departures on runway 4 vs. JFK arrivals on runway 4 | –0.737 | 0.293 | –2.51 |
| LGA departures on runway 22 vs. JFK departures on runway 13 | –1.15 | 0.312 | –3.68 |
| LGA arrivals on runway 22 vs. JFK arrivals on runway 13 | 0.85 | 0.308 | 2.76 |
| LGA arrivals on runway 31 vs. JFK arrivals on runway 13 | 1.27 | 0.464 | 2.75 |
| LGA arrivals on runway 13 vs. JFK departures on runway 13 | –1.99 | 0.224 | –8.88 |
| LGA arrivals on runway 4 vs. JFK arrivals on runway 13 | –0.448 | 0.172 | –2.6 |
| LGA arrivals on runway 13 vs. JFK arrivals on runway 13 | –1.61 | 0.222 | –7.26 |
| LGA arrivals on runway 31 vs. JFK arrivals on runway 13 | 0.796 | 0.25 | 3.19 |
| LGA arrivals on runway 13 vs. JFK departures on runway 4 | –2.5 | 0.341 | –7.34 |
| LGA arrivals on runway 22 vs. JFK arrivals on runway 4 | –0.737 | 0.293 | –2.51 |
| LGA arrivals on runway 4 vs. JFK departures on runway 13 | –1.15 | 0.312 | –3.68 |

the estimated weights indicate that inertia is, as expected, the most important factor when a runway configuration is being selected at LGA, particularly for Configurations 22|31 and 22, 31|31.

In addition, the results indicate that the headwind parameters are statistically significant for the primary arrival runway but not for the primary departure runway or the extra arrival runway. This finding seems to suggest that the alignment of the primary arrival runway is more important than the alignment of the departure or extra arrival runways. This relative importance could result from the fact that aircraft arrivals must be served whereas departures can be held under extreme conditions. Furthermore, the negative influence of tailwinds was found to be statistically significant in all cases. The high headwind variable for the primary arrival runway had a slightly lower value than the normal headwind variable, a difference suggesting that high headwinds are slightly less preferable because of compression.

Arrival demand effects were statistically significant for the low-capacity Configurations 31|31 and 4|4. During high-demand scenarios, these configurations were less likely to be selected. VMC was seen to be important for Configurations 31|31 and 31|4 and therefore seems to suggest that VMC is an important consideration for arrivals on Runway 31.

Switch proximity was significant for only 10 of 42 possible configuration switches. All had negative values, which represented a resistance to a certain configuration switch. The relative weights suggest that, in general, air traffic control prefers not to reverse the direction of airport operations.

### Prediction of Runway Configuration

As Table 5 shows, the overall prediction accuracy for LGA in 2012 on a 15-min horizon was 97.9% and 81.3% on a 3-h horizon. Similar to those for the SFO prediction model, configurations that were seen more often had a higher relative prediction accuracy. For comparison, prior research using logistic regression models for LGA without any look-ahead achieved a prediction accuracy of 75% at LGA (*12*).

**TABLE 5 Prediction Accuracy for LGA in 2012 for 15-min and 3-h Prediction Horizons**

| Configuration (Arrival\|Departure) | Frequency | Prediction Accuracy (%) | |
|---|---|---|---|
| | | 15 min | 3 h |
| 22\|13 | 7,661 (29%) | 98.2 | 88.3 |
| 22\|31 | 2,705 (10%) | 97.6 | 73.9 |
| 22, 31\|31 | 1,675 (6%) | 96.9 | 68.8 |
| 31\|31 | 2,335 (9%) | 97.0 | 71.9 |
| 31\|4 | 6,448 (25%) | 98.2 | 85.5 |
| 4\|13 | 4,355 (17%) | 98.0 | 79.7 |
| 4\|4 | 875 (3%) | 96.7 | 69.8 |
| Total | 26,054 | 97.9 | 81.3 |

## CASE STUDY: EWR

### Model Specification

In the EWR model, configurations were removed if they were not seen at least in 1% of the decision selection periods throughout the year. Many model structures were tested, and the final resulting model was chosen as a nested logit structure with nests containing all alternatives by using Runway 4 for arrivals, with a scale parameter of $\mu_{ARR4} = 1.22$, as shown in Figure 4.

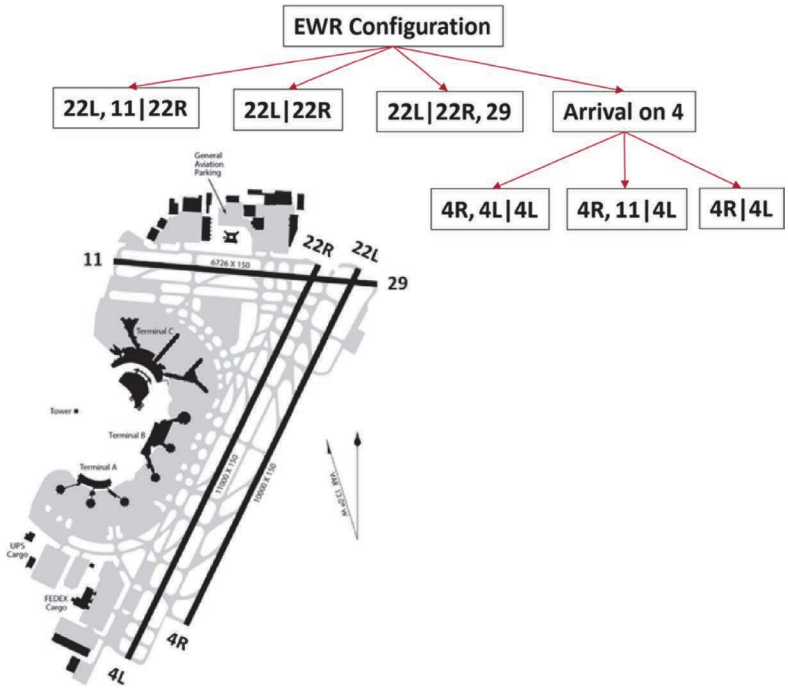


FIGURE 4 EWR model specification.

TABLE 6 Estimated Utility Function Weights for EWR

| Parameter | Value | SE | *t*-Stat. |
|---|---|---|---|
| Inertia Parameters | | | |
| Configuration 22L, 11\|22R | 4.74 | 0.247 | 19.2 |
| Configuration 22L\|22R | 4.74 | 0.247 | 19.2 |
| Configuration 22L\|22R, 29 | 4.74 | 0.247 | 19.2 |
| Configuration 4R, 4L\|4L | 5.12 | 0.431 | 11.86 |
| Configuration 4R, 11\|4L | 5.12 | 0.431 | 11.86 |
| Configuration 4R\|4L | 5.12 | 0.431 | 11.86 |
| Wind Parameters | | | |
| High headwind on arrival runway | 0.104 | 0.0377 | 2.75 |
| Normal headwind on arrival runway | 0.104 | 0.0377 | 2.75 |
| Tailwind on arrival runway | –0.104 | –0.0377 | 2.75 |
| Demand Parameters | | | |
| Arrival demand (thresh ≥ 12) configuration 22L, 11\|22R | 3.33 | 1.12 | 2.95 |
| Arrival demand (thresh ≥ 10) configuration 4R, 4L\|4L | 1.19 | 0.771 | 1.54 |
| Arrival demand (thresh ≥ 10) configuration 4R, 11\|4L | 1.19 | 0.771 | 1.54 |

## Estimated Model and Inferences

The estimated weighting parameters for the utility function for the EWR model are shown in Table 6. Again, inertia is shown as the most important variable to the decision selection. Similar to those for the SFO model, the runway configurations from each nest were grouped under common inertia variables.

Compression effects at EWR were not statistically significant during estimation. In addition, headwinds and tailwinds showed a linear correlation. As a result, the high headwind, normal headwind, and tailwind variables were all linearly constrained in the final model. Similar to those for the LGA model, the wind variables for the departure runways at EWR were not statistically significant, a result that again may indicate that air traffic control prioritizes arrivals over departures when selecting a runway configuration.

Arrival demand was shown as statistically significant for runway configurations with extra arrival runways, namely, 22L, 11|22R; 4R, 4L|4L; and 4R, 11|4L. As arrival demand increased, these configurations received a utility bonus that encouraged the addition of an arrival runway to handle the increasing demand. The threshold values used in the model were determined as a nuisance parameter. Interestingly, a similar variable dealing with the departure demand was not statistically significant for Configuration 22L|22R, 29.

## Prediction of Runway Configuration

As Table 7 shows, the overall prediction accuracy for EWR in 2012 was 97.9% on a 15-min horizon and 78.2% on a 3-h horizon. As with the other models tested, configurations that were seen more often had higher relative accuracies. This general trend seems to suggest that the discrete choice approach may be limited when one is trying to predict runway configurations that are not seen often throughout the year.

## CONCLUSIONS

The nominal process for selecting runway configurations by air traffic control personnel at SFO, LGA, and EWR International Airports was developed by using a discrete choice framework. The models developed for each airport were trained on 2011 data from the ASPM database and were tested by using 2012 ASPM data. Utility functions for different runway configurations that reflect the importance of various factors such as weather, wind speed and direction, airport demand, noise mitigation, interairport coordination, and the incumbent runway configuration were used to develop a probabilistic forecast of the runway configuration on 15-min and 3-h planning horizons.

The weights assigned to the utilities were used to infer the relative importance of the attributes. Across all models, the inertia variables were seen to have the highest importance when the selection decision was being made. In addition, headwinds on arrival runways were also found to be an important factor. For LGA and EWR, high-capacity configurations were favored under high-arrival demand scenarios. At SFO, demand effects were coupled with visibility because of runway separation procedures. Switch proximity reflected a preference to reduce the operational effort required from a runway configuration switch.

The authors performed case studies by using 2012 ASPM data for SFO, LGA, and EWR airports. The models assumed perfect knowledge of weather and airport demand. On a 15-min planning horizon, the SFO, LGA, and EWR models achieved accuracies of 98.2%, 97.9%, and 97.9%, respectively. On a 3-h planning horizon, the models achieved accuracies of 81.2%, 81.3%, and 78.2%, respectively.

TABLE 7 Prediction Accuracy for EWR in 2012 for 15-min and 3-h Prediction Horizons

| Configuration (Arrival\|Departure) | Frequency | Prediction Accuracy (%) | |
|---|---|---|---|
| | | 15 min | 3 h |
| Configuration 22L, 11\|22R | 3,954 (13%) | 96.2 | 58.8 |
| Configuration 22L\|22R | 13,737 (47%) | 98.4 | 82.9 |
| Configuration 22L\|22R, 29 | 157 (1%) | 92.6 | 45.2 |
| Configuration 4R, 4L\|4L | 66 (<1%) | 90.9 | 34.8 |
| Configuration 4R, 11\|4L | 1,303 (4%) | 94.4 | 46.0 |
| Configuration 4R\|4L | 10,191 (35%) | 98.4 | 84.2 |
| Total | 29,408 | 97.9 | 78.2 |

The limitations seen in this study must be acknowledged. Because the approach was data driven, the predictions are limited only to runway configurations that have been previously seen. In addition, runway configurations that are seen infrequently are hard to predict accurately. The proposed models capture nominal behavior; however, realistically, decision makers demonstrate variability, which can be a possible source of error in the results. Furthermore, the Bayesian approach increases any errors or biases in the models for predictions on a 3-h horizon. In many cases, the heavy influence of the inertia parameter will bias the predictions to hold the incumbent configuration even when a switch is preferable.

Despite these limitations, the prediction performance of the proposed discrete choice models suggests that they are a promising approach to predicting runway configuration a few hours ahead of time. On a broad scope, these models could be developed over multiple years of data for all FAA core airports and clustered by weight parameters of similarly defined variables. These models could then be included in future NextGen decision support tools.

Potential areas of future work specific to the models in this paper can also be defined. The inertia term could be improved by limiting its effect as time progresses within a 3-h prediction period. Biases within the estimated parameters could be reduced by estimating the utility parameters with a balanced data set. The effect of wind gusts, which are currently ignored, can also be included in the utility models. Coordination variables could be added for all airports in the New York metroplex for the LGA and EWR models, and full models of JFK and TEB can be developed. Furthermore, new models for SFO could be estimated by defining both a side-by-side and a staggered class for Configuration 28R, 28L|1R, 1L and by using the distributions of airport arrival rates under VMC and IMC in the ASPM data. Challenges will still be present with this type of modeling because side-by-side and staggered operations are not reported in the ASPM data. Preliminary analysis shows that this lack of ground truth will likely lower the overall accuracy of the model to approximately 70%, but new insights on the demand and visibility variables may be present. High-demand scenarios will correlate more heavily with VMC, and low-demand scenarios will correlate significantly with IMC.

## ACKNOWLEDGMENTS

The research in this paper was supported in part by the Transportation Research Board through a Graduate Research Award in Public-Sector Aviation administered by the Airport Cooperative Research Program. The authors thank Monica Alcabin of Boeing, Larry Goldstein of the Transportation Research Board, Belinda Hargrove of TransSolutions, and Renee Hendricks of FAA for their suggestions and guidance. Special thanks go to Sarah Pauls and Mary Sandy of the Virginia Space Grant Consortium for scheduling meetings and facilitating discussions during the entire process.

## REFERENCES

1. Gilbo, E. Airport Capacity: Representation, Estimation, Optimization. *IEEE Transactions on Control System Technology,* Vol. 1, No. 3, 1993, pp. 144–153.
2. Enhanced Preferential Runway Advisory System (ENPRAS). Flight Transportation Associates, 2001. http://www.ftausa.com/enpras.htm.
3. Southgate, D. G., and S. J. Sedgwick. Time Stamped Aircraft Noise Prediction: Replacing the "Average Day" with the "Composite Year." Presented at Inter-Noise 2006, Honolulu, Hawaii, Dec. 2006.
4. Li, L., and J.-P. Clarke. A Stochastic Model of Runway Configuration Planning. Presented at AIAA Guidance, Navigation and Control Conference, Toronto, Ontario, Canada, Aug. 2010.
5. Provan, C. A., and S. C. Atkins. Optimization Models for Strategic Runway Configuration Management Under Weather Uncertainty. Presented at 10th AIAA Aviation Technology, Integration, and Operations (ATIO) Conference, Fort Worth, Texas, 2010.
6. Weld, C., M. Duarte, and R. Kincaid. A Runway Configuration Management Model with Marginally Decreasing Transition Capacities. *Advances in Operations Research,* 2010.
7. Frankovich, M. J., D. Bertsimas, and A. R. Odoni. Optimal Selection of Airport Runway Configurations. *Operations Research,* Vol. 59, No. 6, Nov.–Dec. 2011, pp. 1407–1419.
8. Oseguera-Lohr, R., N. Phojanamongkolkij, G. Lohr, and J. W. Fenbert. Benefits Assessment for Tactical Runway Configuration Management Tool. Presented at AIAA Aviation Technology, Integration, and Operations (ATIO) Conference, Los Angeles, Calif., Aug., 2013.
9. Liu, P.-C. B., M. Hansen, and A. Mukherjee. Scenario-Based Air Traffic Flow Management: From Theory to Practice. *Transportation Research Part B,* Vol. 42, 2008, pp. 685–702.
10. Buxi, G., and M. Hansen. Generating Probabilistic Capacity Profiles from Weather Forecast: A Design-of-Experiment Approach. Presented at 9th USA–Europe Air Traffic Management (ATM2011) Research and Development Seminar, Berlin, 2011.
11. Hesselink, H., and J. Nibourg. Probabilistic 2-Day Forecast of Runway Use: Efficient and Safe Runway Allocation Based on Weather Forecast. Presented at 9th USA–Europe Air Traffic Management (ATM2011) Research and Development Seminar, Berlin, 2011.
12. Houston, S., and D. Murphy. Predicting Runway Configurations at Airports. Presented at 91st Annual Meeting of the Transportation Research Board, Washington, D.C., 2012.
13. Ramanujam, V., and H. Balakrishnan. Estimation of Maximum-Likelihood Discrete-Choice Models of the Runway Configuration Selection Process. Presented at American Control Conference, San Francisco, Calif., June–July 2011.
14. Ramanujam, V., and H. Balakrishnan. Data-Driven Modeling of the Airport Configuration Selection Process. *IEEE Transactions on Human–Machine Systems,* Vol. 45, No. 4, 2014, pp. 490–499.
15. Ben-Akiva, M., and S. Lerman. *Discrete Choice Analysis: Theory and Application to Travel Demand.* MIT Press, Cambridge, Mass., 1985.
16. Bierlaire, M. Biogeme: A Free Package for the Estimation of Discrete Choice Models. Presented at 3rd Swiss Transport Research Conference, Ascona, Switzerland, 2003.
17. Bertsekas, D., and J. Tsitsiklis. *Introduction to Probability,* 2nd ed. Athena Scientific, Belmont, Mass., 2008.
18. Aviation System Performance Metrics (ASPM) database. FAA, U.S. Department of Transportation. aspm.faa.gov.
19. DeLaura, R. A., R. F. Ferris, F. M. Robasky, S. W. Troxel, and N. K. Underhill. *Initial Assessment of Wind Forecasts for Airport Acceptance Rate (AAR) and Ground Delay Program (GDP) Planning.* Report ATC-414. Lincoln Laboratory, Cambridge, Mass., Jan. 2014.
20. *Airport Capacity Benchmark Report.* FAA, U.S. Department of Transportation, 2004.
21. Airport Noise and Emissions Regulations. Boeing Co. www.boeing.com /commercial/noise/san francisco.html.
22. Ganoung, B., and D. Ong. Noise Abatement. San Francisco International Airport. http://www.boeing.com/resources/boeingdotcom/commercial /noise/san_francisco.html.

*The ACRP Selection Panel for the Graduate Research Award Program on Public-Sector Aviation Issues peer-reviewed this paper.*